Influence of pH on Ce IV -[As III W 9 O 33] 9– association for the formation of hexanuclear cerium(iv) oxo-hydroxo-clusters stabilized by trivacant polyanions

Maxime Dufaye, Sylvain Duval, Gregory Stoclet, Thierry Loiseau

Influence of the pH for the Ce^{IV} - $[As^{III}W_9O_{33}]^{9-}$ association to the formation of hexanuclear cerium(IV) oxo-hydroxo-clusters stabilized by trivacant polyanions.

Maxime Dufaye[†], Sylvain Duval[†,*], Gregory Stoclet[‡] and Thierry Loiseau[†]

Contribution from [†]Université de Lille, CNRS, Centrale Lille, ENSCL, Univ. Artois, UMR 8181 – UCCS – Unité de Catalyse et Chimie du solide, F-59000 Lille, France [‡] Unité Matériaux et Transformation (UMET) – UMR CNRS 8207, Université de Lille Nord de France, USTL-ENSCL, Bat C6, BP 90108, 59652 Villeneuve d'Ascq, France.

[*] To whom correspondence should be addressed. E-mail: sylvain.duval@univ-lille.fr. Phone: (33) 3 20 434 973, Fax: (33) 3 20 43 48 95.

Version November 26, 2019

Abstract: Four hetero-polyoxometalate compounds were obtained in aqueous solution, following the synthetic combination of $Na_9[B\text{-}\alpha\text{-}As^{III}W_9O_{33}]$ with the 4f tetravalent cerium cation, in the presence of formate ligand at different pH values (ranging from 1.5 to 6). Each of these four molecules $[\{Ce_6(\mu^3\text{-}O)_4(\mu^3\text{-}OH)_4(HCOO)_{3,5}\}_4(As^{III}W_9O_{33})_4]^{2-}$ compound **1**, $[(Ce_6(\mu^3\text{-}O)_4(\mu^3\text{-}OH)_4)(H_2O)_4(As^{III}W_9O_{33})(HCOO)_9]^{6-}$ compound **2**, $[(Ce_6(\mu^4\text{-}O)_3(\mu^3\text{-}O)_5(\mu^2\text{-}H_2O)_3(HCOO)_3(As^{V}W_9O_{34})_3]^{22-}$ compound **3** and $[(W_4O_{10})\{(Ce_6(\mu^3\text{-}O)_5(\mu^4\text{-}O)_3(\mu^2\text{-}H_2O))(As^{V}W_9O_{34})_3\}_2]^{44-}$ compound **4** are constructed around one to four hexanuclear cerium clusters of $[Ce_6O_8]$ type. For the compounds **1-3**, the arsenato-polytungstate POM units and formate ligands are associated and participate in the stabilization of one cerium(IV)-bearing hexanuclear unit in a cyclic motif (**1**), a monomeric POM species for **2**, and a trimeric POM species for **3**. However, in the last molecular system (**4**), only inorganic entities are bonded to the hexameric cerium(IV) clusters. From the structural point of view, compound **4** appears as the association of two compound **3** entities, in which the formate ligands have been replaced by an inorganic tungsten-based sub-unit, coming from the partial decomposition of the $\{As^{III}W_9O_{33}\}$ precursor. The behavior and the association modes of the four molecular species are explained on the basis of the pH variation used for their syntheses. All four compounds have been characterized by single-crystal X-ray diffraction, IR spectroscopy, TGA and SEM/EDX microscopy and ICP analyses. Solution behavior was assessed on compound **3** by using Small Angle X-ray Scattering (SAXS) measurements.

Keywords: polyoxometalate, cerium(IV), SAXS, pH controlled condensation.

1. Introduction

The studies of polyoxometalates gain an extraordinary increasing interest in the last decades due to their capacities to act as ligands (related to the nucleophilicity of the oxygen atoms encircling the vacancies) and complex a wide range of electrophilic species. This association gives them a great structural diversity form which results in many properties in various scientific fields.[1–7] These compounds are built up from polycondensation processes of oxo-metalates, either under acidic or basic conditions, depending on the nature of the metal-oxo species involved. One sub-class of these molecules, namely the heteropolyoxometalates are constructed by polycondensation of the metalates around a templating agent, either being tetrahedral (XO_4, X = P^V, Si^V, Ge^V, *etc.*) or trigonal (XO_3, X = As^{III}, Sb^{III}, Bi^{III}, *etc.*). As an example of this diversity with transition metals, one may mention for instance, the review of Mialane, Dolbecq *et al.*[8,9] and Proust *et al.*[6] describing a great number of diverse topologies. Surprisingly, the investigations of the complexation of tetravalent heavy elements (for instance: cerium, uranium, thorium) remain particularly less explored. As a consequence, we have been interested for several years by the understanding of the condensation process of these 4f and 5f elements and how to control the formation of polynuclear oxo-clusters. Two strategies were employed in our laboratory. The first one, also developed by other research teams, concerns the use of organic oxo-donor ligands (carboxylic acids or amino acids) with a control of the quantity of added water (to allow condensation) in organic solvents and leads to interesting molecular species with high nuclearity, up to 38 atoms for tetravalent actinides or 40 atoms for cerium.[10–13]

The second strategy was focused on is the use of polyvacant polyoxometalates. They are able to act as ligands in water and, with benefits of monotopic carboxylic acids, which help to control the condensation of the versatile tetravalent cations. By using this strategy, we have been able to isolate several fascinating systems with original shapes and nuclearity, starting from the trivacant silicotungstate $\{SiW_9O_{34}\}$ polyanion.[14] In the case of tetravalent cerium (which can be used as a surrogate for tetravalent radionuclides), pH modulation and stoichiometric variation on the number of added cations results in the formation of several moieties with up to twelve cerium(IV) centers complexed by polyanion and ligand moieties.[15–17] The same strategy with actinide elements also gives rise to very remarkable architectures with unexpected behavior.[18,19] Very recently, a peroxo-route was also developed to stabilized polyanionic species incorporating cerium(IV) cations for catalytic purposes.[20]
Herein we report on the synthesis of four distinct molecular entities obtained by varying the synthesis pH ranging from 1.5 to 6, in presence of a molar excess of cerium (ca. 5 eq) with the trivacant $\{As^{III}W_9O_{33}\}$ polyanion and formic acid. The single-crystal XRD structural analyses show the presence of hexanuclear cerium(IV)-centered polyoxo/hydroxo clusters stabilized by mixtures of trivacant polyanion and formate ligands. For two of the four molecules, the supposed stable As(III) center in $\{As^{III}W_9O_{33}\}$ was found to be oxidized in As(V) state to form in situ the $\{As^{V}W_9O_{34}\}$ unit.

2. Experimental section

Synthesis.
The starting chemical reactants ($(NH_4)_2Ce^{IV}(NO_3)_6$, Fisher Scientific, 99%; formic acid, Aldrich, 99%; sodium formate, Aldrich, 99%; NH_4NO_3, Aldrich, 99%) are available commercially and were used without any further purification. $Na_9[AsW_9O_{33}]\bullet 12H_2O$ has been prepared from the synthesis protocol described in inorganic synthesis volume 27.

*Compound **1***. $(NH_4)_2Ce^{IV}(NO_3)_6$ (255 mg, 0.465 mmol) and $Na_9[AsW_9O_{33}]\bullet 12H_2O$ (250 mg, 0.093 mmol) were dissolved in 10 mL of a 1 M formic acid aqueous solution. The pH of the mixture was measured at 1.5. The resulting solution was heated at 70°C for 30 minutes and was then cooled to room temperature resulting in the precipitation of a yellow powder that was eliminated by centrifugation to give a clear orange-yellow solution. After 1 week, small prismatic yellow crystals suitable for X-ray diffraction analyzes started to appear. The crystals were filtered off after one more week before apparition of an amorphous phase and dried at room temperature (m = 31 mg, yield = 10 % based on W). The pH of the remaining solution was still at 1.5.
IR (cm^{-1}): 946(w), 866(w), 849(m), 782(m), 659(m), 563(m).
ICP-OES for $Na_2[\{Ce_6(\mu^3\text{-}O)_4(\mu^3\text{-}OH)_4(HCOO)_{3,5}\}_4(AsW_9O_{33})_4]\cdot 76H_2O$: Na (0.37%), As (2.01%), W (44.5%), Ce (22.9%). Calculated: Na (0.31%), As (2%), W (44.3%), Ce (22.5%).

*Compound **2***. $(NH_4)_2Ce^{IV}(NO_3)_6$ (0.255 mg, 0.465 mmol) was dissolved in 10 mL of HCOOH/HCOONa 1M buffer. $Na_9[AsW_9O_{33}]\bullet 12H_2O$ (250 mg, 0.093 mmol) was added to the cerium aqueous solution under stirring. The pH of the solution was 3.7. The resulting

mixture was heated at 70°C for 30 minutes. The solution was cooled to room temperature and centrifuged to remove a yellow powder and the resulting solution was left to crystallize by slow evaporation. After a few days, orange crystals suitable for X-ray diffraction analyzes started to appear. The crystal were collected, washed with a small amount of cold water and dried at room temperature (m = 114 mg, yield = 37 % based on W). The pH of the remaining solution was measured at 3.5.
IR (cm^{-1}): 938 (w), 834(m), 780(s), 685(m), 641(s), 542(s).
ICP-OES for $Na_6[(Ce_6(\mu^3\text{-}O)_4(\mu^3\text{-}OH)_4)(H_2O)_4(AsW_9O_{33})(HCOO)_9]\cdot 7H_2O$: Na (3.1%), As (2.1%), W (43.8%), Ce (22.9%). Calculated: Na (3.5%), As (1.9%), W (41.9%), Ce (21.2%).

Compound ***3***. $(NH_4)_2Ce^{IV}(NO_3)_6$ (255 mg, 0.465 mmol), $Na_9[AsW_9O_{33}]\bullet 12H_2O$ (250 mg, 0.093 mmol) and NH_4NO_3 (28 mg, 0.35 mmol) were dissolved in 10 mL of a HCOOH/HCOONa buffered aqueous solution adjusted at pH = 5 by NaOH addition. The mixture was then heated at 70 °C for 30 minutes, cool to room temperature and centrifuged. The clear yellow solution was placed in an oven at 80°C for 12 hours. After this time, crystals suitable for X-Ray diffraction analyses were obtained and collected (m = 37 mg, yield = 12 % based on W). The pH of the remaining solution was measured at 4.3.
IR (cm^{-1}): 950(w), 861(w), 840(w), 775(m), 711(m), 647(m).
ICP-OES for $Na_{22}[(Ce_6(\mu^4\text{-}O)_3(\mu^3\text{-}O)_5(\mu^2\text{-}H_2O)_3)(HCOO)_3(As^VW_9O_{34})_3]\cdot 63H_2O$: Na (4.7%), As (2.4%), W (49.7%), Ce (8.4%). Calculated: Na (4.9%), As (2.2%), W (48.6%), Ce (8.2%).

Compound ***4***. $(NH_4)_2Ce^{IV}(NO_3)_6$ (255 mg, 0.465 mmol), $Na_9[AsW_9O_{33}]\bullet 12H_2O$ (250 mg, 0.093 mmol) and sodium formate (320 mg, 4.7 mmol) were dissolved in 10 mL H_2O. The solution was adjusted at pH = 6 by NaOH addition. The mixture was then heated at 70 °C for 30 minutes and then cooled to room temperature before centrifugation. The solution was then left to crystallize in an oven at 80°C for 12 hours when few crystals suitable for X-Ray diffraction analyses appeared. (m = 8 mg, yield = 2.9 % based on W). The pH of the remaining solution was measured at 5.5.
IR (cm^{-1}): 949(w), 871(w), 838(w), 774(m), 659(m).
ICP-OES for $Na_{43}[(W_4O_{10})\{(Ce_6(\mu^3\text{-}O)_5(\mu^4\text{-}O)_3(\mu^2\text{-}H_2O))(AsW_9O_{34})_3\}_2].140H_2O$: Na (4.9%), As (2.4%), W (53.9%), Ce (8.7%). Calculated: Na (4.9%), As (2.3%), W (53.4%), Ce (8.4%).

Single-crystal X-ray diffraction. Crystals of compounds **1-4** were selected under polarizing optical microscope and glued on a mitegen loop for a single-crystal X-ray diffraction experiment. X-ray intensity data were collected on a Bruker X8-APEX2 CCD area-detector diffractometer using Mo-K_α radiation (λ = 0.71073 Å) with an optical fiber as collimator. Several sets of narrow data frames (10 s per frames) were collected at different values of θ for two initial values of ϕ and ω, respectively, using 0.3° increments of ϕ or ω. Data reduction was accomplished using SAINT V8.34a.[21] The substantial redundancy in data allowed a semi-empirical absorption correction (SADABS 2014/5) to be applied,[22] on the basis of multiple measurements of equivalent reflections. The structure was solved by direct methods, developed by successive difference Fourier syntheses, and refined by full-matrix least-squares on all F^2 data using SHELX program suite [23] on the OLEX2 graphical tool.[24] The final refinements include anisotropic thermal parameters of all non-hydrogen atoms, except for the

oxygen atoms of the water molecules or other atoms that would be NPD if refined anisotropically. In the lattice, some water molecules were localized but, most of them were highly disordered and thus were squeezed on the four structures. The crystal data of compounds **1-4** are given in Table 1 and some explanations are given on the A level alerts on the section "comments on structure level A alerts" on the supplementary informations. Supporting information is available in CIF format for all compounds (CCDC numbers 1955271, 1955272, 1955273 and 1955274 for compounds **1**, **2**, **3** and **4** respectively).

Thermogravimetric analysis. The thermogravimetric experiments for compounds **1**-**4** have been carried out on a thermoanalyzer TGA 92 SETARAM under air atmosphere with a heating rate of 1°C.min^{-1} from room temperature up to 800°C.

Infrared spectroscopy. Infrared spectra of compounds **1**-**4** were measured on Perkin Elmer Spectrum Two^{TM} spectrometer between 4000 and 400 cm^{-1}, equipped with a diamond Attenuated Total Reflectance (ATR) accessory. No ATR correction was applied to the measured spectra.

SEM/EDX Analysis. Photographs of the crystals were performed on a Hitachi Model S3400N system equipped with a tungsten filament. EDX measurements were performed on compounds **1**-**4** to estimate the elemental composition, with respect to the molecular composition, and can be found in the Supporting Information.

Inductively Coupled Plasma Spectroscopy. Crystal of compound **1**–**4** were dissolved in 2% HNO_3 solutions and were analyzed using a Vista-Pro Varian ICP-OES. Each compound was analyzed separately to determine the Na / As / W / Ce ratios. Based on the number of W atoms in each compounds, the percentages of each elements can be estimated.

SAXS measurements. The measurements were performed on a SAXS Xeuss 2.0 apparatus (Xenocs) equipped with a micro source using a Cu K_α radiation (λ = 1.54 Å) and point collimation (beam size: 300 x 300 μm^2). The sample to detector distance, around 35cm, is calibrated using silver behenate as standard. The analyzed solutions are placed in 1.5 mm glass capillaries at a concentration of about 25 mmol.L^{-1}. Before the analyses of each measurement, the contribution of the glass capillaries and the solvent is subtracted using a reference containing the solvent according to standard procedures.
The experimental scattering curves were compared to those of simulated scattering model, computed by the SolX software starting from the CIF files of the compound.[25–27]

3. Results

Synthesis. The synthesis of these four compounds was performed in aqueous solution by mixing a stable trivacant polyanion, $[As^{III}W_9O_{33}]^{9-}$ with an excess of CAN (Cerium Ammonium Nitrate, ca. 5 equivalents) in presence of formic acid / sodium formate at pH

values ranging from 1.5 to 6. This strategy was made to force a greater amount of cerium to interact into the vacancies of the polyanionic ligand $[As^{III}W_9O_{33}]^{9-}$. It gives rise to the formation of crystalline solids for all four molecules presented in this contribution (Figure S1). Above pH 6, no coloration of the centrifuged solution was observed and a large amount of amorphous solid appeared, indicating the probable precipitation of all cerium(IV) containing compounds. As previously described in some related systems, the association of the inorganic polyanionic moieties with organic oxo-donor ligands is an interesting approach to control the polycondensation of tetravalent cations, cerium for instance and, confine it to polynuclear clusters (under tetranuclear or well-known hexanuclear units). We were first surprised to observe the formation of crystals when working at a low pH value of 1.5. In these conditions, polyoxometalates are not always stable. This reaction medium does not favor the condensation formation of polynuclear cationic species, as it generally requires hydroxyl ions for the condensation process to occur. Nevertheless, some recent solutions and kinetics studies support the occurrences of polynuclear cerium(IV)-centered clusters, albeit in quite different conditions but, at very low pH values (approximately pH = 0 in nitric acid).[28–31] These drastic conditions for the polyanionic moieties may explain the low yield of compound **1**. In the case of compounds **3** and **4**, the reason probably lies in the synthesis itself, where a large amount of yellow unidentified precipitate is formed, reducing the quantity of molecules present in the solutions left for crystallization. Nevertheless, pH measurements after removal of the crystals (4.3 and 5.5 respectively for compounds 3 and 4) indicate the presence of a condensation process of the cerium cations during the synthesis. It could explain the large amount of fine yellow precipitate formed during these two compounds synthesis.

Structure description. Compound **1** crystallizes in a tetragonal $I\bar{4}$ space group while the three other molecules **2 - 4** are organized in a triclinic $P\bar{1}$ space group. All four compounds appear to stabilize one or several hexanuclear cerium(IV) oxo/hydroxo clusters by means of some formate ligands. In **1**, the asymmetric unit is constituted by one $\{As^{III}W_9O_{33}\}$ polyanion, one $\{Ce_6\}$ hexanuclear cerium cluster and four formate ligands. The complete molecular system is then obtained by application of a 4-fold-axis and one inversion center. In this molecule, the $\{As^{III}W_9O_{33}\}$ and $\{Ce_6\}$ building units are alternated to form a crown-like association (Figure 1a).

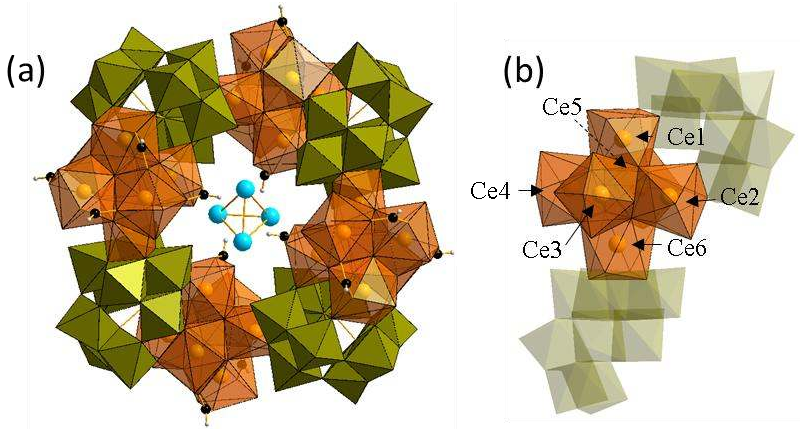

Figure 1: (a) Structural representation of the crown like association in compound **1** and (b) highlight and labels of the cerium cluster. $\{WO_6\}$: green polyhedron, $\{CeO_n, n=8\text{-}9\}$: orange polyhedron, C: black spheres, Na: blue spheres and H: white spheres.

The cerium-based cluster is constituted by five cations (Ce1, Ce2, Ce4, Ce5 and Ce6) with a coordination number of VIII related to a square-based antiprismatic geometry. A sixth cerium center (Ce3) adopts a coordination number of IX with a mono-capped square-based antiprismatic geometry (Figure 1b). BVS calculations on the six cerium centers confirm their tetravalent oxidation state (Table S2).[32] The Ce-O bonds distances lie in the classical range and the oxygen atoms come from different elements of the molecule. Indeed, the cerium centers are found to be bound to oxygen atoms from the polyoxometalate ($Ce\text{-}O_{POM}$ = 2.317(12) Å – 2.471(12) Å), terminal water molecules ($Ce\text{-}O_{H_2O}$ = 2.391(12) Å – 2.626(15) Å), formate ligands ($Ce\text{-}O_{form}$ = 2.363(14) Å – 2.421(15) Å) and oxo/hydroxo bridges ($Ce\text{-}O_{oxo/hydroxo}$ = 2.173(12) Å – 2.524(12) Å) inherent to the hexameric cluster. The structural analysis shows that the hexamer has the composition $\{Ce_6(\mu^3\text{-}O)_4(\mu^3\text{-}OH)_4\}$ frequently observed in the literature. Indeed, shorted Ce-O bond lengths (2.173(12) Å – 2.257(12) Å) are assigned to the four μ^3-oxo groups, whereas longer Ce-O bond lengths (2.356(12) Å – 2.524(12) Å) are related to four μ^3-hydroxo groups. This typical and particular configuration was previously reported in many hexanuclear oxo/hydroxo clusters with cerium(IV) interacting in POM species[16] or carboxylates for instance.[33–40] In the case of carboxylates, they can acts as hexameric clusters nodes for the construction of MOFs type materials. In our case, the organic part of compound **1** is constituted of formate ligands. On each hexamers, three ligands are fully present and a fourth one appears to be present with occupancy close to 0.5. They adopt a bidentate bridging mode with two adjacent cerium centers. Consequently, for the four cerium hexamers present on the molecular motif, a total of fourteen formate ligands are localized. Finally, two sodium cations disordered on four positions organized around a tetrahedral geometry (with an occupancy factor of 0.5), appear to be embedded within the inorganic cycle with Na-O distances of 2.67(2) Å. Surprisingly, these two cations are the only counter-charge present on the crystal lattice of this molecule, which exhibits a complete formula $Na_2[\{Ce_6(\mu^3\text{-}O)_4(\mu^3\text{-}OH)_4(HCOO)_{3,5}(AsW_9O_{33})\}_4]\cdot yH_2O$. The -2 charge for a molecule constructed around several polyoxometalate is relatively rare and can explain its aqueous insolubility for further solution studies.

The second compound (**2**) of this series is relatively close from the one described above. A close structural examination reveals that the molecular motif is constructed by the association of a cerium(IV) hexamer interacting with one $\{As^{III}W_9O_{33}\}$ species and eight formate ligands (Figure 2a). This hexanuclear unit is different from the precedent one as only four cerium atoms (Ce3, Ce4, Ce5 and Ce6) have a coordination number of VIII (with a square antiprism geometry). The two other ones (Ce1 and Ce2) possess a higher coordination number of IX with the mono-capped square antiprismatic environment as in compound **1** (Figure 2b).

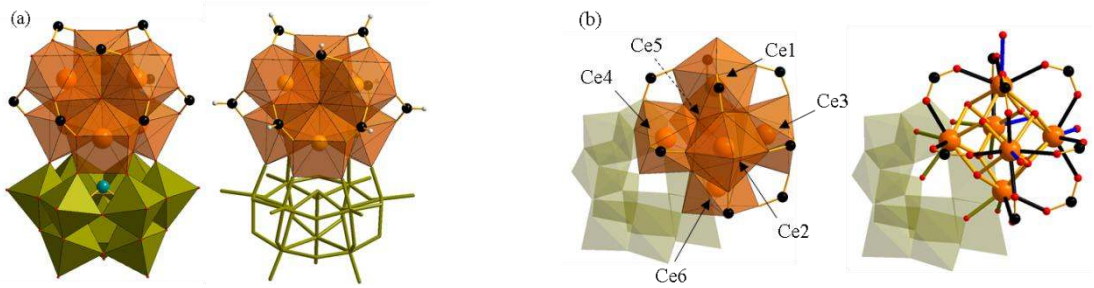

Figure 2: (a) Structural representation of compound **2** and (b) highlight and labels of the cerium cluster. {WO_6}: green polyhedron, {CeO_n, n=8-9}: orange polyhedron, C: black spheres, Na: blue spheres and H: white spheres. Ce-O bonds with the polyanion are in green, with the formate ligands in black, with the central oxo/hydroxo bridges in orange and with water in blue.

The BVS calculations confirm the tetravalent state of the cerium cations (See Table S2). The Ce-O distances in the hexamer are comparable to those found in compound **1**. The Ce-O_{POM} distances lie in the range 2.30(2) Å – 2.33(2) Å, the Ce-$O_{formate}$ distances range between 2.39(2) Å and 2.51(2) Å, the Ce-$O_{oxo/hydroxo}$ are comprised between 2.17(2) Å and 2.49(2) Å and, the Ce-O_{H_2O} distances are of about 2.43(3) Å to 2.62(2) Å. Considering the oxo/hydroxo bridges between the cerium centers, the hexamer has the classic composition {$Ce_6(\mu^3\text{-}O)_4(\mu^3\text{-}OH)_4$}, with typical shorter bond lengths (2.17(2) Å – 2.27(2) Å) for the μ^3-oxo groups and longer bond lengths (2.40(2) Å – 2.49(2) Å) for the μ^3-hydroxo groups. We were also able to locate all the counter cations in the crystal lattice. Five sodium cations have been found to compensate the charges of the polyanionic moieties and, the complete formula of compound **2** is then deduced as $Na_5[(Ce_6(\mu^3\text{-}O)_4(\mu^3\text{-}OH)_4)(H_2O)_4(AsW_9O_{33})(HCOO)_8]\cdot yH_2O$. As observed for compound **1**, this relatively low charge could also explain the low solubility of this molecule.

Compounds **3** and **4** crystallize in the $P\bar{1}$ space group. These two molecules are structurally close since several similarities can be noticed when looking at the molecular arrangement (Figure 3).

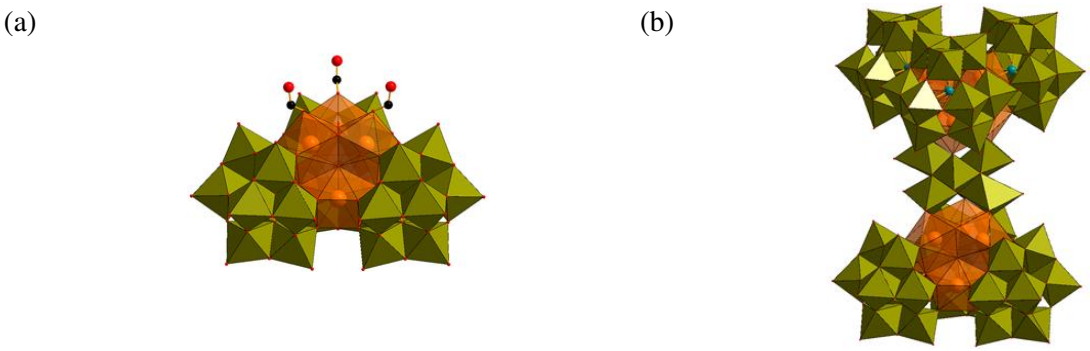

Figure 3: Polyhedral representation of compound **3** (a) and compound **4** (b). {WO_6}: green polyhedrons, {CeO_n, n=8-9}: orange polyhedrons, As: blue-green sphere, C: black sphere and O: red sphere.

At a first glance, compound **4** appears to be a dimerization of compound **3**, where the two monomers are linked by an additional oxo-tungstic moiety replacing the terminal formate ligands capping the hexanuclear cerium-based cluster of the compound **3**.

Both molecules **3** and **4**, are built up from the complexation of cerium(IV) hexameric clusters (confirmed by BVS calculations, See table S2) stabilized by trivacant polyanionic moieties with a 1:3 hexamer/polyanion ratio. In each hexamer of compounds **3** and **4**, three cerium cations (labelled Ce4, Ce5 and Ce6) have a coordination number of VIII (square-based antiprismatic geometry) and, are linked by the polyanionic entities. The three others (labelled Ce1, Ce2 and Ce3) have a coordination number of IX (mono-capped square-based antiprismatic geometry). They correspond to the three centers linked either to the formate ligands in compound **3** or to an additional oxo-tungstic group in compound **4**. This sub-unit of tungsten centers is crystallographically partially disordered with two distinct positions: one is central (multiplicity 2) and fully occupied; the other corresponds to two peripheral positions (multiplicity 2) with a partial occupancy of 30% / 70% (Figure 4). Due to the occurrence of the inversion center, the resulting formula of this tungstate-based oxo-cluster is thus $\{W_4O_{10}\}$.

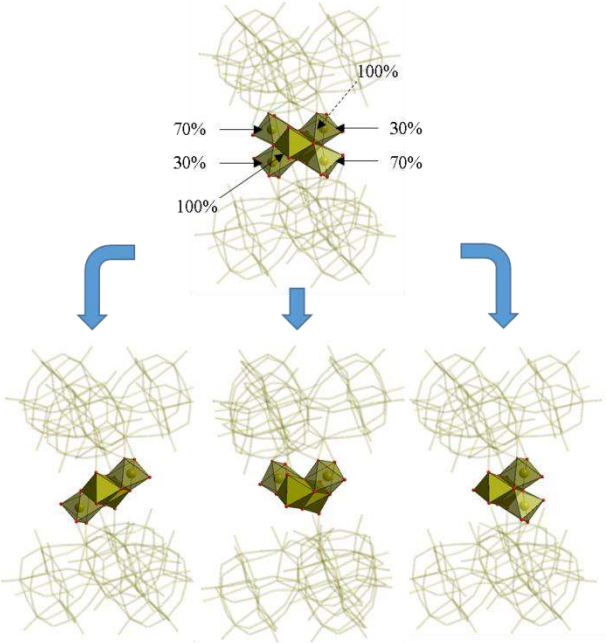

Figure 4: Occupancy factors and statistical disorder on the $\{W_4O_{10}\}$ oxo-tungstic sub-group in compound **4**.

In the cerium(IV)-containing hexamers, classical Ce-O distances are observed with the polyanionic moieties (dist. Ce-O =2.2931(1) Å – 2.3661(2) Å) and surprisingly, the classical 4 μ^3-oxo and 4 μ^3-hydroxo bridges generally present in $\{Ce_6O_8\}$ hexamers are replaced here by 8 $\mu^{3/4}$-oxo bridges (3 μ^4-O and 5 μ^3-O) with Ce-O_{oxo} = 2.104(14) Å – 2.774(16) Å). It is worth noting that the long Ce-O distances, at around 2.7 Å belong to the interactions with the μ^4-oxygen atoms coming from the oxidation of the arsenic(III) into arsenic(V) centers within the polyanionic precursor entities (see the explanations below). It results in a tetrahedral coordination for the arsenic center, with the occurrence of an additional oxygen atom, which adopts a bridging mode with the cerium atoms. The coordination sphere of the nine-fold coordinated cerium centers in compound **3** is completed by three oxygen atoms from three distinct monodentate formate ligands, with Ce-O distances comprised between 2.3949(1) Å and 2.4197(2) Å. As stated above, in compound **4**, the formate ligands are replaced by an oxo-tungstic group interacting through mixed Ce-O bond distances going from 2.334(17) Å to 2.777(18) Å.

One interesting fact is the oxidation of the central As(III) cations in the As(V) oxidation state in both systems. It leads to the formation of the $[B\text{-}\alpha\text{-}As^{V}W_9O_{34}]^{9-}$ polyanion from the $[B\text{-}\alpha\text{-}As^{III}W_9O_{33}]^{9-}$ precursor without any modifications of its isomerism. The As^{V}-O bonds distances in $\{As^{V}W_9O_{34}\}$ ($d_{As(V)\text{-}O}$ = 1.665(10) Å – 1.717(12) Å) appear to be shortened of about 0.1 Å in comparison with the As^{III}-O distances observed in the $\{As^{III}W_9O_{33}\}$ moieties ($d_{As(III)\text{-}O}$ = 1.730(15) Å – 1.809(12) Å). The oxidation of this cation was unexpected and could explain why the amount of polyanionic entities bounded to the central cerium(IV) hexameric clusters is increased, in comparison with the situation in compounds **1** and **2**, for which the POM/$\{Ce_6O_8\}$ ratio is strictly equal to 1. Indeed, the oxidation of the arsenic provides one supplementary oxygen atom to the vacancy of the polyanion, resulting in the increasing number of possible interactions of the $\{As^{V}W_9O_{34}\}$ building block. Thus, the three supplementary oxygen atoms of the tetrahedrally coordinated arsenic(V) from three distinct $\{As^{V}W_9O_{34}\}$ bricks, are linking to one cerium(IV) hexamer in compounds **3** and **4**. Two of the $\{AsO_4\}$ units are connected to cerium(IV) centers having a coordination number of VIII while the third one is linked to a cerium(IV) atom possessing a coordination number of IX (See Figure S2). The oxidation of this cation ($E°(As^{5+}/As^{3+})$ = 0.58 V/NHE) is probably due to the presence of an excess of cerium(IV) which is known to be a strong oxidizing agent ($E°(Ce^{4+}/Ce^{3+})$ = 1,44 V/NHE). Furthermore, it was not observed in compound **1** and **2**, probably because of the longer heating time (80°C for 12 hours in an oven, instead of 70°C for 30 minutes for **1** and **2**) used for the synthesis of the compounds **3** and **4**, activating the redox reaction.

Finally, the negative charges of both compounds are compensated by 22 and 43 sodium cations, which have been hardly observed from single-crystal XRD analysis but fully determined by EDS and ICP measurements. They give a complete structural formula of $Na_{22}[(Ce_6(\mu^4\text{-}O)_3(\mu^3\text{-}O)_5(\mu^2\text{-}H_2O)_3(HCOO)_3(As^{V}W_9O_{34})_3]\cdot yH_2O$ and $Na_{44}[(W_4O_{10})\{(Ce_6(\mu^3\text{-}O)_5(\mu^4\text{-}O)_3(H_2O))(As^{V}W_9O_{34})_3\}_2]\cdot yH_2O$ for compounds **3** and **4**, respectively.

Structural discussion. All the four compounds **1**-**4** possesses a hexanuclear cerium(IV) poly-oxo/hydroxo cluster. A detailed examination of these hexamers shows some differences that can be related to the synthetic conditions (Figure 5).

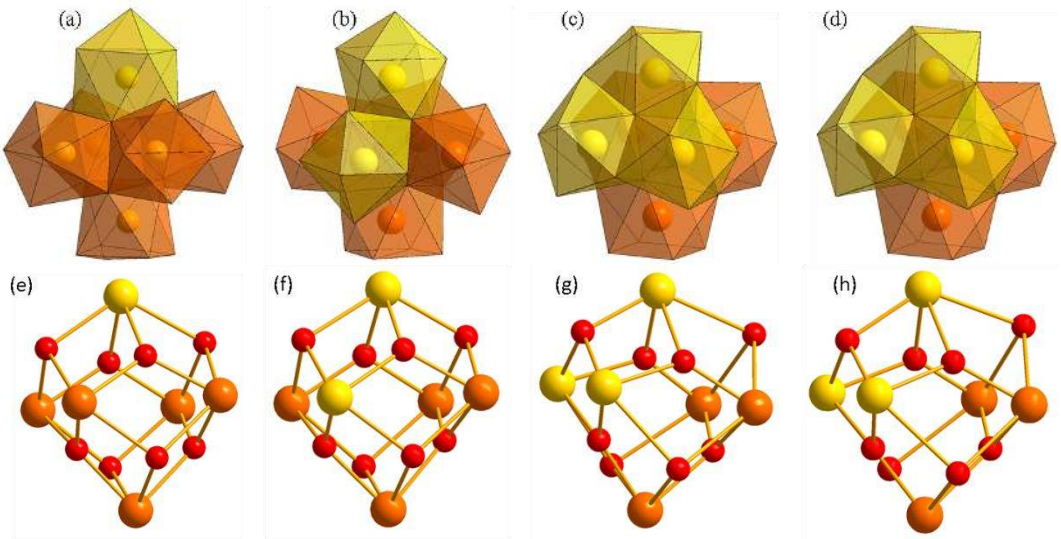

Figure 5: highlight on the hexamers (a-d) and on the $\{Ce_6O_8\}$ core (e-h) in compound **1** (a, e),

compound **2** (b, f), compound **3** (c, g) and compound **4** (d, h). {CeO_8 groups}: orange polyhedra and {CeO_9 groups}: yellow polyhedra. Eight-fold cerium in orange and nine-fold cerium in yellow.

Within the hexamer, the coordination around the cerium(IV) centers seems to fit with the available bridging oxygen atoms from the arsenato-polytungstate moieties, which mainly differ from the oxidation state of the arsenic atom, via either the {$As^{III}O_3$} or {$As^{V}O_4$} units. For compounds **1** and **2**, there are only one or two nine-fold coordinated cerium atoms, with a mono-capped square antiprism geometry. The {CeO_9} and {CeO_8} polyhedra are connected to each other's by single common edges via the μ_3-oxo/hydroxo bridges. On the other hand, in compounds **3** and **4**, the presence of the supplementary oxygen atoms coming from the oxidation of the {$As^{III}O_3$} in {$As^{V}O_4$} groups increase the number of cerium(IV) centers being nine-fold coordinated to oxygen atoms. In addition, their geometry is also different and forms tricapped prismatic polyhedron, which appears to be more flexible than the square antiprismatic ones. These nine-fold polyhedra interact together through two additional adjacent edges. In addition, if we consider the cerium centers to be on the corner of an octahedron, the two groups of cerium elements (eight- and nine-fold coordinated) are organized in a "*facial*" configuration, i. e. they occupy one face of the octahedron. As represented on the ball and stick model of the {Ce_6O_8} cores (Figure 5(e)-(h)), we can see the presence of the three μ^4-O bridges considerably distort the "octahedral" symmetry of the core but, it intrinsically remains on a {Ce_6O_8} state.

In these four molecules, the comparison of the cerium/polyanion ratio shows two tendencies. For **1** and **2**, this ratio is equal to 6 while it is equal to 2 for compound **3** and **4**. The two first systems were obtained at quite low pH values. At pH = 3.5, the formate ligands are more complexing (due to their deprotonation state close to the pKa value of formic acid) towards the cerium cations and thus occupied most of the free oxo positions left on the cerium(IV)-centered hexamer to form a simple molecular adduct. However, at pH = 1.5, they are probably less complexing as most of them are protonated allowing the cerium(IV) hexamers to interact with a neighboring polyanionic entity to form this molecular ring-like compound. From a topological point of view, these two molecules are constructed around the same building block {(AsW_9O_{33})-$(Ce_6O_4(OH)_4)$} which is repeated four times in compound **1**. In the two other molecules, compound **4** could be viewed as a dimerization of compound **3**. At pH = 5, the formate ligands are fully deprotonated and complex the three upper nine-fold coordinated cerium(IV) cations of the hexamers in a monodentate η^1 way. The formate ligands cannot bridge two monomers due to the steric hindrance that would arise between terminal oxo groups of the two polyanionic moieties. At the slightly higher pH value of 6, a competition arises with the formation of complexing oxo-tungstic {W_4O_{10}} groups (coming from the partial decomposition of the polyanionic precursor in our synthetic conditions) that remove these formate ligands to bridge two cerium(IV)-based hexanuclear units. The synthesis of these four molecules highlights the flexible capacities of the trivacant {$AsW_9O_{33/34}$} polyanion to form miscellaneous species.

Infrared spectroscopy. Infrared spectra of compounds **1-4** were measured and compared with the one of the polyanionic precursor $Na_9[B\text{-}\alpha\text{-}AsW_9O_{33}]\cdot 12H_2O$ (Figure 6).

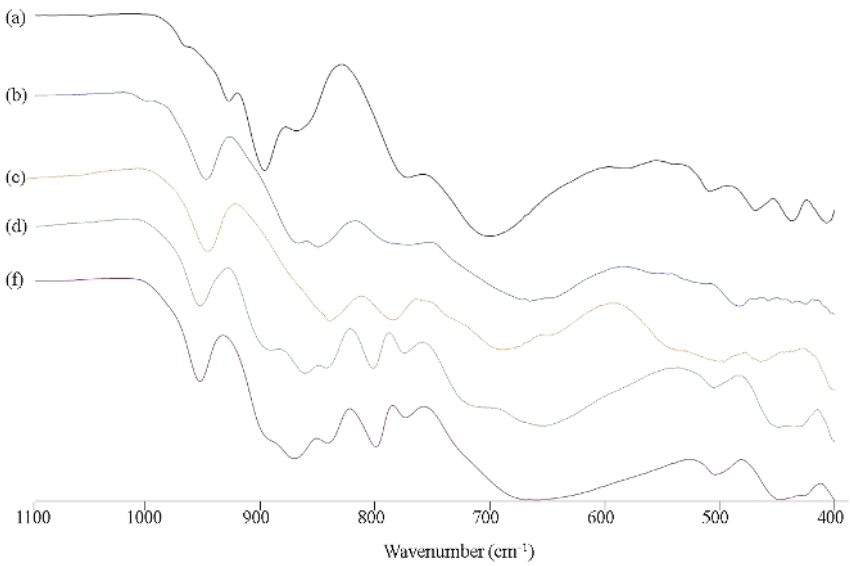

Figure 6: Infrared spectra of $Na_9[B\text{-}\alpha\text{-}AsW_9O_{33}].12H_2O$ (a), compound **1** (b), compound **2** (c), compound **3** (d) and compound **4** (e) in the 1100 - 400 cm^{-1} domain.

The coordination of the cerium(IV) cation to the $\{AsW_9O_{33/34}\}$ polyanionic precursor results in a drastic change in the shape of the IR spectra. The vibrations related to the distinct W-Ox bonds (x = d for terminal oxo groups attached to tungsten centers; x = b for bridging oxo groups between two adjacent tungsten trimers; x = c for bridging oxo groups in a tungsten trimer) are listed in table S4. For instance, the W=Od vibrations at 928 cm^{-1} on the polyanionic precursor is strongly red shifted of about 20 to 30 cm^{-1} in all four compounds. The W-Ob-W vibrations are also modified for the four molecules. The band at 866 cm^{-1} is still present for all spectra as the intrinsic architecture of the polyanionic precursor is not completely modified. However, a second vibration band is visible at around 830-850 cm^{-1} showing the interaction of the oxygen atoms of the vacancies with the cerium centers. Two W-Oc-W vibrations are visible in each compound: one is located at 775 cm^{-1} and is not affected with almost any shifts while the second broad peak at 700 cm^{-1} is much more disturbed by the complexation of the cerium(IV) cations with a blue shift of about 40 cm^{-1}. The presence of the formate ligands in compound **1**, **2** and **3** is confirmed with C=O and C-H vibrations at 1680 cm^{-1} and 1360 cm^{-1} respectively (Figure S3). No C-OH vibrations were observed on the spectra. Nevertheless, no signal at around 1700 cm^{-1}, related to the protonated state of formic acid is observed, indicating that only formate groups occurs at the periphery of the hexanuclear cerium(IV)-based brick.

Thermic behavior. Thermogravimetric analyses were performed on the compounds **1**-**4** in order to determine their water and organic molecules content (Figure 7).

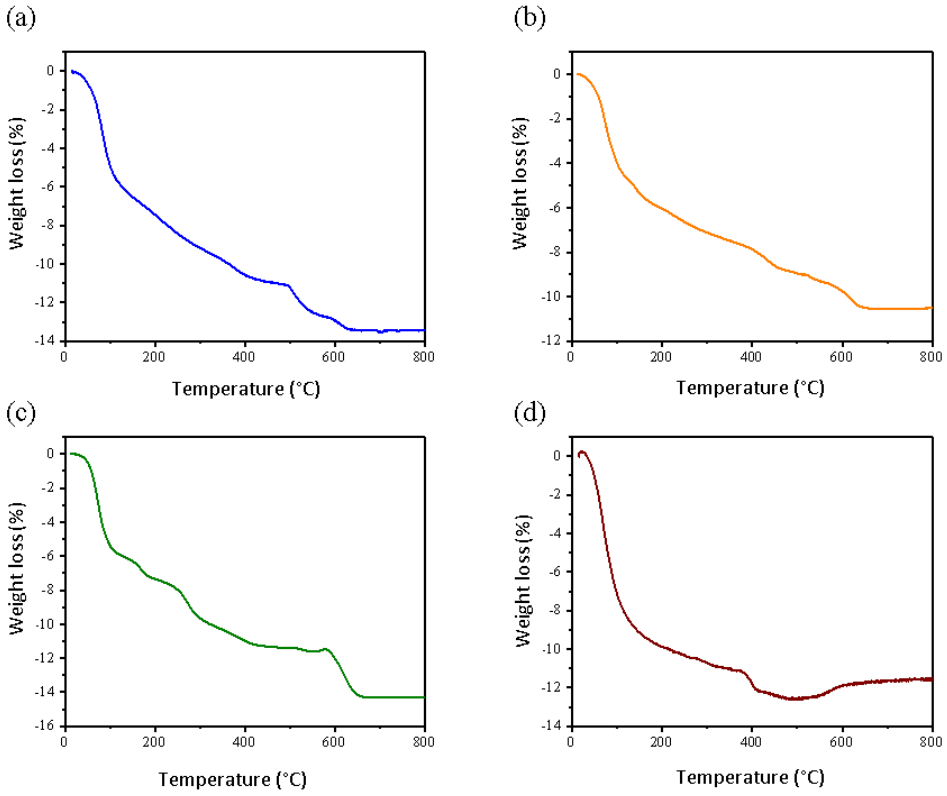

Figure 7: Thermogravimetric analyses of compounds **1** (a), **2** (b), **3** (c) and **4** (d) from room temperature to 800°C (under air atmosphere, 5°C.min^{-1}).

For the water content, calculations were carried out based on the observation of the first loss of weight (stopped around 250°C - 300°C for all compounds) and compared with the number of water molecules located from the single-crystal X-ray diffraction studies. They indicated that the four molecules contain 69 (obs.: 8.7%; X-ray calc.: 8.6%), 7 (obs.: 7%; X-ray calc.: 6.6%), 63 (obs.: 10.4%; X-ray calc.: 9.1%) and 140 (obs.: 10.7%; X-ray calc.: 9.9%) hydration water molecules for compound **1-4**, respectively. The presence of the formate ligands was also confirmed by a second plateau appearing until 400°C. The calculations carried out show the presence of 14 (obs.: 4,9%; X-ray calc.: 5,2%), 7 (obs.: 2,5%; X-ray calc.: 2,9%) and 3,8 (obs.: 1,3%; X-ray calc.: 1,0%) for compounds **1-3** respectively. All these calculated values appear to be in relatively close agreement with the quantity of water and formate ligands localized on the four crystal structures from XRD analyses.
Finally, residual oxides As_2O_5, WO_3, CeO_2 and Na_2O are obtained at 800°C for compounds **1-4**. The theoretical weight of these oxides is 12932 g.mol^{-1}, 3403 g.mol^{-1}, 8271 g.mol^{-1} and 17469 g.mol^{-1} for compounds **1-4** respectively. Using the complete formula weight with the water content of the four molecules, we were able to calculate a molar weight of 14962, 3970, 9588 and 20038 for compounds **1-4** respectively. Thus, the percentages of the weight of the oxide in comparison with the complete mass of the compounds (ca. 86.4%, 85.7%, 86.3% and 87.2%) are close to the remaining percentages observed at 800°C on the four TGA measurements (i.e. 86.5%, 89.5%, 86% and 88% for **1-4** respectively).

Solution studies. In order to estimate the stability of the four molecular systems in aqueous solution, we carried out SAXS (Small angle X-ray Scattering) analysis, which has been

previously reported in literature for the characterization of molecular inorganic polyoxometalate-like species.[41–44] The strategy lies on the dissolution of a given amount of crystalline products of the different compounds **1**-**4** in water, poured in a 1.5 mm diameter glass capillary, with the targeted concentration of 25 mmol.L^{-1}. Unfortunately, in the case of compounds **1** and **2**, and probably due to their relatively low charge (i. e. -2 and -5 for compound **1** and **2**, respectively), we were not able to solubilize their crystals sufficiently to get an exploitable SAXS signal. The extremely low yield (around 3% - based on W) of compound **4** also prevented us to run the SAXS experiment efficiently. Due to these different issues, we could only study the structural behavior of dissolved crystals of compound **3** in an aqueous solution.

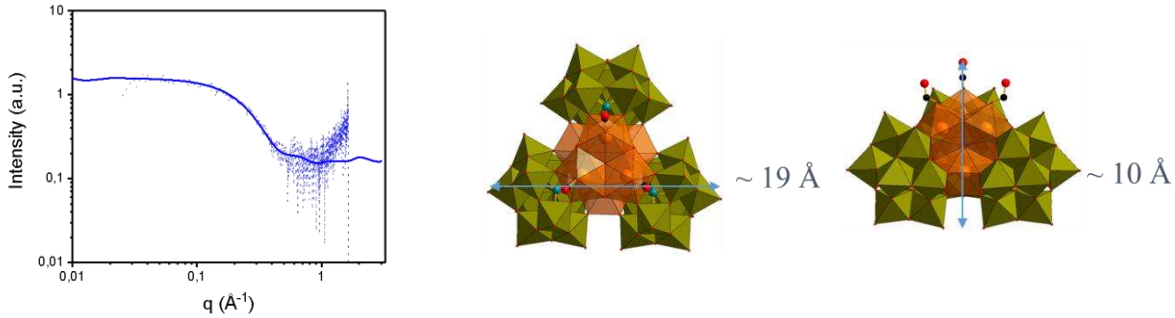

Figure 8: Left: SAXS measurement of compound **3** in water. Experimental data (blue dots) and simulated curve (strong blue line). Right: dimensions of compound **3**.

The SAXS curve is presented in Figure 8, with a specific evolution in the region for $q < 0.8$ $Å^{-1}$. In this range, we used the atomic positions list coming from the XRD model of $Na_{22}[(Ce_6(\mu^4\text{-}O)_3(\mu^3\text{-}O)_5(\mu^2\text{-}H_2O)_3(HCOO)_3(As^VW_9O_{34})_3]\cdot 63H_2O$ in order to simulate a scattering curve (see experimental section). We notice that the two experimental and calculated curves match very well. We also observe a good agreement of the intensity decrease of the SAXS signal, in the range $0.2\ Å^{-1} < q < 0.4\ Å^{-1}$, indicating that the structural parameters of the motif found in compound **3**, are maintained in solution. From a spherical model, it can be deduced a gyration radius (*Rg*) of about 8.5 Å (i.e diameter value of 17 Å) for the dissolved polynuclear species. From the X-ray diffraction, the diameter of three arsenato-polytungstates surrounding the hexanuclear cerium-based cluster is around of 19 Å width and and 10 Å high (Figure 8). Indeed, these values fits well with the calculated one obtained by the SASX experiment, since it is quite close to the biggest diameter reported for the molecular motif in **3**. It reflects that compound **3** is probably stable after dissolution in water and its structural integrity is therefore conserved.

4. Conclusion

We have successfully used the stable trivacant $\{As^{III}W_9O_{33}\}$ polyoxometalate to bind tetravalent cerium cations and build a new series of four distinct compounds (**1**-**4**) incorporating up to six cerium cations per polyanionic moieties, within a $\{Ce_6O_8\}$ cluster. The reaction pH is the main driving force leading to these molecular systems as it plays a

significant role in the protonation state of the formic acid, and consequently influence the coordination strength of these organic ligands.
These four molecules are constituted of one to four hexanuclear cerium(IV) oxo/hydroxo clusters with either VIII or IX coordination numbers, which is quite unusual in tetravalent cerium hexameric bricks of $\{Ce_6O_8\}$ type. This difference is probably due to the oxidation reaction occurring for the formation of compounds **3** and **4**, which transforms the central arsenic atoms of the $\{As^{III}W_9O_{33}\}$ precursor from the $\{As^{III}\text{-}O_3\}$ into $\{As^{V}\text{-}O_4\}$ unit, increasing the number of complexation sites of the vacancies of the polyoxometalates, with an additional available oxo bridge.
The behavior of compound **3** could be reasonably studied by SAXS measurements. It confirms the stability of the molecular entity in aqueous solution. The solubility or low yield of the reaction prevented us to assess the solution behavior of the three other molecules.
We are actually studying other carboxylic ligands trying to get informations on the strength of the acid coordination on the nuclearity of the tetravalent cerium clusters stabilized in presence of trivacant polyanions.

Supplementary informations. Comments on the level A alerts for compounds **1-4**. Crystal data and structures refinement parameters for compounds **1-4** (Table S1). BVS calculations for the cerium and arsenic atoms in compounds **1-4** (Table S2) and for tungsten atoms in compounds **3** and **4** (Table S3). IR values of the main vibrations (in cm^{-1}) of the $Na_9[AsW_9O_{33}]\bullet 12H_2O$ precursor with compounds **1-4** (Table S4). Binocular and SEM images of crystals of compounds **1-4** (Figure S1). Structural highlight of the coordination of the As(V)-O oxygen atoms on the cerium hexamers of compounds **3** and **4** (FigureS2). Full IR spectra of compound **1-4** and $Na_9[AsW_9O_{33}]$ in the region 4000-400 cm^{-1} (Figure S3).

Authors informations.
E-mail: sylvain.duval@univ-lille.fr
ORCID
Maxime Dufaye: 0000-0002-5270-4718
Sylvain Duval: 0000-0002-3398-2501
Grégory Stoclet: 0000-0003-1510-0234
Thierry Loiseau: 0000-0001-8175-3407

Acknowledgment. The authors would like to thank Mrs. Nora Djelal for her technical assistance with the TGA measurements (UCCS). Chevreul Institute (FR 2638), Ministère de l'Enseignement Supérieur, de la Recherche et de l'Innovation, Hauts-de-France Region and FEDER are acknowledged for supporting and funding partially this work. S.D. would like to thanks the ANR for the funding of the POMAR project.

References.

1 M. T. Pope, Y. Jeannin and M. Fournier, *Heteropoly and Isopoly Oxometalates*, Springer Berlin, Berlin, 2013.

2 M. T. Pope and A. Müller, *Angew. Chem. Int. Ed.*, 1991, **30**, 34–48.

3 M. T. Pope and A. Müller, Eds., *Polyoxometalates: From Platonic Solids to Anti-Retroviral Activity*, Springer Netherlands, Dordrecht, 1994, vol. 10.

4 C. L. Hill, *Chem. Rev.*, 1998, **98**, 1–390.

5 D.-L. Long, R. Tsunashima and L. Cronin, *Angew. Chem. Int. Ed.*, 2010, **49**, 1736–1758.

6 A. Proust, B. Matt, R. Villanneau, G. Guillemot, P. Gouzerh and G. Izzet, *Chem. Soc. Rev.*, 2012, **41**, 7605–7622.

7 M. T. Pope and U. Kortz, *Encyclopedia of inorganic and bioinorganic chemistry*, 2011.

8 A. Dolbecq, E. Dumas, C. R. Mayer and P. Mialane, *Chem. Rev.*, 2010, **110**, 6009–6048.

9 O. Oms, A. Dolbecq and P. Mialane, *Chem. Soc. Rev.*, 2012, **41**, 7497–7536.

10 C. Falaise, C. Volkringer, J.-F. Vigier, A. Beaurain, P. Roussel, P. Rabu and T. Loiseau, *J. Am. Chem. Soc.*, 2013, **135**, 15678–15681.

11 N. P. Martin, C. Volkringer, N. Henry, X. Trivelli, G. Stoclet, A. Ikeda-Ohno and T. Loiseau, *Chem. Sci.*, 2018, **9**, 5021–5032.

12 L. Chatelain, R. Faizova, F. Fadaei-Tirani, J. Pécaut and M. Mazzanti, *Angew. Chem. Int. Ed.*, 2019, **58**, 3021–3026.

13 K. J. Mitchell, K. A. Abboud and G. Christou, *Nat. Commun.*, 2017, **8**, 1445.

14 S. Duval, S. Béghin, C. Falaise, X. Trivelli, P. Rabu and T. Loiseau, *Inorg. Chem.*, 2015, **54**, 8271–8280.

15 S. Duval, P. Roussel and T. Loiseau, *Inorg. Chem. Commun.*, 2017, **83**, 52–54.

16 S. Duval, X. Trivelli, P. Roussel and T. Loiseau, *Eur. J. Inorg. Chem.*, 2016, **2016**, 5373–5379.

17 M. Dufaye, S. Duval, K. Nursiah, G. Stoclet, X. Trivelli and T. Loiseau, *CrystEngComm*, 2018, **20**, 7144–7155.

18 M. Dufaye, S. Duval, G. Stoclet, X. Trivelli, M. Huvé, A. Moissette and T. Loiseau, *Inorg. Chem.*, 2019, **58**, 1091–1099.

19 M. Dufaye, S. Duval, G. Stoclet and T. Loiseau, *Eur. J. Inorg. Chem.*, 2019, **42**, 4500–4505.

20 H. M. Qasim, W. W. Ayass, P. Donfack, A. S. Mougharbel, S. Bhattacharya, T. Nisar, T. Balster, A. Solé-Daura, I. Römer, J. Goura, A. Materny, V. Wagner, J. M. Poblet, B. S. Bassil and U. Kortz, *Inorg. Chem.*, 2019, **58**, 11300–11307.

21 *Brucker Analytical X-ray Systems: Madison, WI, 2008*, 2014.

22 G. M. Sheldrick, *Brucker-Siemens Area detector Absorption and Other Correction*, 2015b.

23 G. M. Sheldrick, *Acta Crystallographica Section A Foundations of Crystallography*, 2008, **64**, 112–122.

24 O. V. Dolomanov, L. J. Bourhis, R. J. Gildea, J. A. K. Howard and H. Puschmann, *J. Appl. Crystallogr.*, 2009, **42**, 339–341.

25 F. Förster, B. Webb, K. A. Krukenberg, H. Tsuruta, D. A. Agard and A. Sali, *J. Mol. Biol.*, 2008, **382**, 1089–1106.

26 J. L. O'Donnell, X. Zuo, A. J. Goshe, L. Sarkisov, R. Q. Snurr, J. T. Hupp and D. M. Tiede, *J. Am. Chem. Soc.*, 2007, **129**, 1578–1585.

27 X. Zuo, G. Cui, K. M. Merz, L. Zhang, F. D. Lewis and D. M. Tiede, *Proc. Natl. Acad. Sci.*, 2006, **103**, 3534–3539.

28 M. R. Antonio, R. J. Ellis, S. L. Estes and M. K. Bera, *Phys. Chem. Chem. Phys.*, 2017, **19**, 21304–21316.

29 M. R. Antonio, T. J. Demars, M. Audras and R. J. Ellis, *Sep. Sci. Technol.*, 2018, **53**, 1834–1847.

30 T. J. Demars, M. K. Bera, S. Seifert, M. R. Antonio and R. J. Ellis, *Angew. Chem. Int. Ed.*, 2015, **54**, 7534–7538.

31 H. Feuchter, S. Duval, C. Volkringer, F.-X. Ouf, L. Rigollet, L. Cantrel, M. De Mendonca Andrade, F. Salm, C. Lavalette and T. Loiseau, *ACS Omega*, 2019, **4**, 12896–12904.

32 P. L. Roulhac and G. J. Palenik, *Inorg. Chem.*, 2003, **42**, 118–121.

33 M. Lammert, M. T. Wharmby, S. Smolders, B. Bueken, A. Lieb, K. A. Lomachenko, D. D. Vos and N. Stock, *Chem. Commun.*, 2015, **51**, 12578–12581.

34 V. Mereacre, A. Ako, M. Akhtar, A. Lindemann, C. Anson and A. Powell, *Helv. Chim. Acta*, 2009, **92**, 2507–2524.

35 R. Das, R. Sarma and J. B. Baruah, *Inorg. Chem. Commun.*, 2010, **13**, 793–795.

36 P. Toledano, F. Ribot and C. Sanchez, *C. R. Acad. Sci.*, 1990, **311**, 1315–1320.

37 G. Lundgren, *Arkiv Kemi*, 1956, **9**, 183–197.

38 A. Buragohain and S. Biswas, *CrystEngComm*, 2016, **18**, 4374–4381.

39 R. Dalapati, B. Sakthivel, A. Dhakshinamoorthy, A. Buragohain, A. Bhunia, C. Janiak and S. Biswas, *CrystEngComm*, 2016, **18**, 7855–7864.

40 R. Dalapati, B. Sakthivel, M. K. Ghosalya, A. Dhakshinamoorthy and S. Biswas, *CrystEngComm*, 2017, **19**, 5915–5925.

41 M. Nyman, *Coord. Chem. Rev.*, 2017, **352**, 461–472.

42 L. Ruhlmann and D. Schaming, Eds., *Trends in polyoxometalates research*, Nova Publishers, New York, 2015.

43 J. N. Wacker, M. Vasiliu, I. Colliard, R. L. Ayscue, S. Y. Han, J. A. Bertke, M. Nyman, D. A. Dixon and K. E. Knope, *Inorg. Chem.*, 2019, **58**, 10871–10882.

44 P. C. Burns and M. Nyman, *Dalton Trans.*, 2018, **47**, 5916–5927.